

Alternative nonlinear-optical expansion and diagrammatic approach: Nth-order dephasing-induced effects

Rick Trebino

Combustion Research Facility, Sandia National Laboratories, Livermore, California 94550

(Received 12 January 1988)

We show that dephasing-induced nonlinear-optical effects whose amplitudes are proportional to trinomials of dephasing rates, $\Gamma_{ij} + \Gamma_{jk} - \Gamma_{ik}$, exist in all nonlinear orders of perturbation theory. To do this, we derive a new form for the perturbation expansion of the susceptibility, equivalent to the currently used expansion, but which writes each order as a sum of (1) terms due to single-sided diagrams, and (2) correction terms, *all of which are proportional to trinomials of dephasing rates*. The proof of this result utilizes a diagrammatic approach involving a new type of double-sided diagram for the latter terms. These diagrams immediately yield the terms proportional to trinomials of dephasing rates in all orders without the need for algebraic manipulation. This approach also reveals some general properties of the Nth-order susceptibility.

I. INTRODUCTION

While expressions for the nonlinear-optical susceptibility that correctly incorporate damping have existed for over 20 years,^{1,2} only a decade ago did researchers discover in them the class of "dephasing-induced" or "pressure-induced" resonances.³ One reason for this delay is that the full expression for $\chi^{(3)}$ for a four-level system, for example, contains 1152 terms, although if the sum over all state permutations is not performed, the number of terms falls to 48. Not surprisingly, even the 48-term expression was not explicitly written down until 1977.⁴ It was then that the required algebraic manipulation of this expression was performed to reveal the class of dephasing-induced resonances.³

These nonlinear-optical resonances have zero or nearly zero strength in the absence of collisional dephasing because the two or more quantum-mechanical amplitudes potentially contributing to signal radiation add coherently and cancel out. In the presence of collisional dephasing, however, these amplitudes cease to cancel out, resulting in resonances whose strength increases with pressure. An example of a dephasing-induced effect is a resonance between initially unpopulated states.^{3,5} After algebraic manipulation of the third-order terms that contain these initially-unpopulated-state resonances, their strengths are seen to be proportional to trinomials of dephasing rates:³

$$\Gamma_{ijk} \equiv \Gamma_{ij} + \Gamma_{jk} - \Gamma_{ik}, \quad (1)$$

where $\Gamma_{\alpha\beta}$ is the total dephasing rate between states α and β . Typically, this quantity vanishes when pure dephasing can be neglected, i.e., when the pressure is zero. When pure dephasing cannot be neglected, an approximately linear pressure dependence results. Prior *et al.*⁶ have observed such a resonance between the $3P_{3/2}$ and $3P_{1/2}$ levels of sodium.

Several other third-order dephasing-induced phenomena have been observed experimentally. Bloembergen and co-workers have observed collisional-dephasing-induced

population gratings^{7,8} and collisional-dephasing-induced resonances between equally populated ground electronic states (hyperfine and Zeeman levels).^{9,10} Grynberg and co-workers have demonstrated dephasing-induced oscillation^{11,12} and self-focusing.¹³ Additional processes that have been shown to have dephasing-induced components, and which have been observed, include coherent emission between different initially unpopulated excited electronic states,¹⁴ fluorescence,¹⁵⁻¹⁷ saturation spectroscopy,¹⁸ and the Hanle effect.¹⁹⁻²¹

Extension of this work to higher order and to saturation regimes has also begun. Grynberg's⁵ dressed-state calculations have revealed dephasing-induced resonances between initially unpopulated states even in the presence of strong two-photon coupling. Furthermore, even in this regime, the resonance amplitude retains its proportionality to Γ_{ijk} . Agarwal and co-workers²²⁻²⁴ have calculated expressions for dephasing-induced effects in the presence of saturating fields and have shown that dephasing-induced effects exist in higher-order wave mixing. In addition, researchers have experimentally observed higher-order dephasing-induced resonances. Dagenais^{25,26} has observed a $2\omega_1 - \omega_2$ process, resonant between populated excited states, using a collisional-redistribution process to populate these states, which yielded an overall fifth-power dependence on intensity. Trebino and Rahn^{27,28} have seen subharmonics of hyperfine resonances, which appear to be due to dephasing-induced nonlinearities at least as high order as $\chi^{(13)}$. Agarwal²⁴ has modeled subharmonics with a two-oscillator model, a dressed-state picture, and higher-order perturbation theory. Of these three approaches, the last is, perhaps, the most intuitive because subharmonics are clearly evident in higher-order perturbation-theory diagrams.²⁸⁻³⁰ Thus these experiments would benefit from a higher-order perturbation-theory treatment. Indeed, it would be useful in general to understand the nature of dephasing-induced phenomena in all orders of the perturbative nonlinear susceptibility.

In their original paper, Bloembergen *et al.*³ performed

algebraic manipulations of the second- and third-order perturbative susceptibilities, which led them to discover dephasing-induced processes in those orders. Working with expressions for these susceptibilities that correctly included damping (rather than incorrectly including it by allowing frequencies to become complex in the final result), they rearranged terms. For the 48-term expression for $\chi^{(3)}$, for example, they obtained another 48-term expression, which contained two types of terms. It contained the 24 terms usually obtained by neglecting damping until the final result. (We will refer to these terms as the “principal terms” because they adequately describe most of the nonlinear-optical processes that have been observed to date, see Sec. III.) It also contained 24 “correction terms” proportional to trinomials of dephasing rates, Γ_{ijk} . All resonances between initially unpopulated states occurred in these latter terms.

In order to understand higher-order dephasing-induced effects, it would be useful to perform analogous algebraic manipulations for higher orders. The number of terms in the N th-order susceptibility increases as $2^N N!$, however. It is thus apparent that, in higher order, the algebraic manipulation required to separate out terms whose strength depends on dephasing becomes much more complex. The problem is that the usual nonlinear-optical perturbation expansion involves a one-to-one correspondence between terms and quantum-mechanical propagators.^{29,30} This expansion is physically intuitive, but it cannot conveniently describe dephasing-induced resonances, which in $\chi^{(3)}$ necessarily involve partial sums of more than one propagator.³ Thus, to best describe dephasing-induced phenomena in all orders, an expansion that involves appropriate rearrangements of potentially very many terms is required.

In this paper we perform this rearrangement in all orders and describe the new perturbation expansion for the nonlinear-optical susceptibility that results. This new expansion is equivalent to the currently used expansion,^{29,30} valid in the impact approximation, assuming isolated lines, monochromatic radiation, steady-state operation, and no initial system coherence. It reveals dephasing-induced phenomena with amplitudes proportional to trinomials of dephasing rates, Γ_{ijk} , in all orders and has the advantage that it explicitly displays the terms proportional to Γ_{ijk} in all orders—no algebraic manipulation is necessary to obtain them. Specifically, in this expansion, the nonlinear-optical susceptibility is written as the sum of (1) principal terms, obtainable from single-sided diagrams^{31,32} and (2) correction terms, all of which are proportional to trinomials of dephasing rates, Γ_{ijk} . As a result, we also refer to the correction terms as “trinomial-dephasing terms.” We find that, as the order increases, trinomial-dephasing terms dominate the expression for the susceptibility in the sense that their relative fraction of the total number of terms approaches unity.

The proof of these statements involves a new diagrammatic approach for writing down the above expansion for the nonlinear-optical susceptibility. This approach uses single-sided diagrams to yield the principal terms and a new type of double-sided diagram, which we call a “trinomial-dephasing diagram,” to yield the correction

terms. The latter type of diagram yields dephasing-induced effects proportional to a trinomial of dephasing rates directly and immediately *in any order*, without the need for algebraic manipulation.

The expansion and corresponding diagrammatic approach are not only useful for the above proof, but in addition, they also appear useful for understanding the nonlinear susceptibility in general. They may also be useful for calculations.

II. BACKGROUND AND NOMENCLATURE

Several authors^{29,30,33,34} describe general (“integral”) approaches to writing the N th-order density matrix as sums of time-ordered N -dimensional integrals over propagators and perturbation Hamiltonians, correctly including damping. Most calculations of theoretical expressions, however, require a few simplifying assumptions. Typically, one assumes the impact approximation, monochromatic radiation, isolated spectral lines, steady-state operation, negligible population transfer, and zero initial values for off-diagonal density-matrix elements.^{29,30,35} We will refer to these approximations as the “standard approximations.” These approximations allow the relaxation of the off-diagonal density-matrix elements, ρ_{ij} , to be written as $\exp(-\Gamma_{ij}t)$, where Γ_{ij} , the total dephasing rate, is given by

$$\Gamma_{ij} = \frac{1}{2}(\gamma_i + \gamma_j) + \Gamma_{ij}^{\text{pd}}. \quad (2)$$

In this expression, γ_i and γ_j are the longitudinal relaxation rates (including decay due to spontaneous emission and inelastic collisions³⁶) of levels i and j , respectively, and Γ_{ij}^{pd} is the pure dephasing rate between levels i and j .^{30,35} These approximations allow the time-ordered N -dimensional integrals over the propagators and Hamiltonians to be performed. As a result, each propagator yields a resonant denominator of the form $1/[\omega_{ij} - (\sum_i \omega_i) - i\Gamma_{ij}]$, where ω_{ij} is a transition frequency and $\sum_i \omega_i$ is a sum of up to N input light frequencies. Bloembergen,¹ Lynch,⁴ and Flytzanis² have written down expressions for the N th-order nonlinear-optical susceptibility within these approximations.

Whether the standard approximations are made or not, a double-sided diagrammatic approach can be used to describe the terms in the expression for the N th-order nonlinear-optical susceptibility. Bordé and co-workers³³ describe diagrammatic approaches for the integral expressions (and for other problems^{33,34}); Yee and co-workers^{29,30} and Omont *et al.*³⁵ give descriptions of diagrammatic interpretations in both regimes; and Prior³⁷ reviews the approach under the standard approximations, showing explicitly all 48 of the diagrams and corresponding terms for $\chi^{(3)}$. Prior³⁷ also describes the relation of double-sided to single-sided diagrams, the latter of which do not correctly describe collisional dephasing.²⁹ The conventions and formalism used by Prior³⁷ will be adopted in this paper, as we also work within the standard approximations.

We include here a note on nomenclature. In addition to collisional dephasing, dephasing due to *longitudinal relaxation* can also lead to noncancelling nonlinear-optical

amplitudes.²⁶ “Decay-induced resonances” have been observed.³⁸ This effect can be seen in trinomial-dephasing terms by separating dephasing due to longitudinal relaxation from pure dephasing using Eq. (2):

$$\Gamma_{ijk} = \gamma_j + (\Gamma_{ij}^{\text{pd}} + \Gamma_{jk}^{\text{pd}} - \Gamma_{ik}^{\text{pd}}) . \quad (3)$$

Thus, unless the lifetime of state j is infinite, there will be a component due to longitudinal relaxation. It is for this reason that we use the general adjective “dephasing induced” instead of the more common terms “pressure induced” or “collision induced,” which ignore this contribution. Additional nomenclature issues arise when we consider that correction terms can add coherently to a resonance that results from one or more principal terms. In this case, dephasing perturbs an already existing resonance, rather than inducing the resonance itself, so that a better noun for the general class of effects might be “phenomena” or “effects.” To further complicate the matter, many third-order nonlinear-optical effects have been shown to be related to the presence of dephasing, although not through Γ_{ijk} terms.^{7–21} Most of these effects have amplitudes proportional to a single dephasing rate Γ_{ij} or to a positive-weighted sum of dephasing rates, without the possibility of cancellation. Consequently, it might be useful to distinguish between these two types of effects. With these points in mind, we henceforth adopt in this work the general names, “dephasing-induced phenomena,” for the general class of effects owing their existence to dephasing and, specifically, “trinomial-dephasing phenomena” for the effects of terms proportional to Γ_{ijk} . We will refer to terms in the nonlinear susceptibility proportional to Γ_{ijk} as “trinomial-dephasing terms,” as mentioned earlier.

III. CORRECTION TERMS IN $\chi^{(3)}$

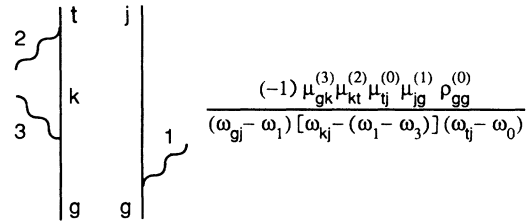
In this section we review the rearrangement of the 48-term expression for $\chi^{(3)}$ due to Bloembergen *et al.*,³ and, using this order as an example, introduce concepts necessary to treat the N th order. Familiarity with the single-sided and double-sided diagrammatic approaches, as reviewed by Prior,³⁷ would be helpful in understanding the discussion that follows.

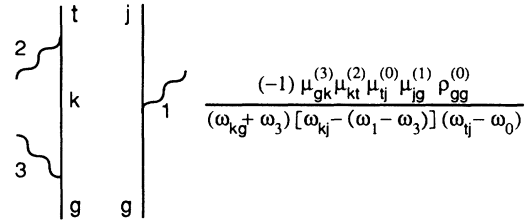
Bloembergen *et al.* observed that, for a given nonlinear-optical process, the expression for $\chi^{(3)}$ contains several triplets of terms with the same dipole-moment and density-matrix elements in their numerators. As a result, each triplet of terms could be algebraically manipulated without reference to a particular atomic or molecular system. For each triplet, they obtained two correction terms, proportional to trinomial-dephasing factors, and a principal term, which could be written using a single-sided diagram.³⁷ Twelve triplets produced 24 correction terms, each proportional to a trinomial-dephasing factor, and 12 principal terms. The remaining 12 terms of the original 48 each have unique products of matrix elements in their numerators and so cannot be manipulated. These last 12 terms result from the remaining 12 single-sided diagrams. Thus the manipulation did not reduce the number of terms in the expression for $\chi^{(3)}$, but it did produce another 48-term expression that con-

tained all of the principal terms (due to single-sided diagrams), plus an equal number of correction terms (all proportional to trinomial-dephasing factors).

We now describe this rearrangement in some detail for a particular process. Consider a four-wave-mixing process of the form $\omega_0 = \omega_1 + \omega_2 - \omega_3$, involving the states g , k , t , and j , with g populated. Figure 1 shows a triplet of double-sided diagrams, having the same matrix elements in their numerators. Also shown in Fig. 1 are the terms resulting from these diagrams. We can algebraically manipulate the three terms in Fig. 1 to yield three new terms that sum to the same value. They consist of the following principal term:

$$\frac{(-1) \mu_{gk}^{(3)} \mu_{kt}^{(2)} \mu_{tj}^{(0)} \mu_{jg}^{(1)} \rho_{gg}^{(0)}}{(\omega_{kg} + \omega_3) [\omega_{tg} - (\omega_2 - \omega_3)] (\omega_{gj} - \omega_1)} , \quad (4)$$





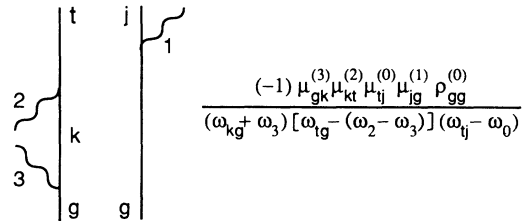


FIG. 1. Three double-sided diagrams and the terms obtained from them for the four-wave-mixing process $\omega_0 = \omega_1 + \omega_2 - \omega_3$. The states are labeled g , k , t , and j ; $\mu_{\alpha\beta}^{(\gamma)}$ is the dipole-moment-matrix element between states α and β for the polarization of the beam at the frequency ω_γ ; and $\rho_{gg}^{(0)}$ is the population density of state g . $\omega_{\alpha\beta}$ is the transition frequency between states α and β . In all diagrammatic approaches considered in this work, all transition frequencies $\omega_{\alpha\beta}$ are understood to be complex, that is, to include the dephasing rate between α and β : $\omega_{\alpha\beta} \rightarrow \omega_{\alpha\beta} - i\Gamma_{\alpha\beta}$. A detailed description of the construction and interpretation of double-sided diagrams is given in Ref. 37.

and two correction terms:

$$\frac{(-1)\mu_{gk}^{(3)}\mu_{kt}^{(2)}\mu_{ij}^{(0)}\mu_{jg}^{(1)}\rho_{gg}^{(0)}(-i\Gamma_{tgi})}{(\omega_{kg} + \omega_3)[\omega_{ig} - (\omega_2 - \omega_3)](\omega_{gj} - \omega_1)(\omega_{ij} - \omega_0)}, \quad (5)$$

$$\frac{(-1)\mu_{gk}^{(3)}\mu_{kt}^{(2)}\mu_{ij}^{(0)}\mu_{jg}^{(1)}\rho_{gg}^{(0)}(-i\Gamma_{kgj})}{(\omega_{kg} + \omega_3)(\omega_{gj} - \omega_1)[\omega_{kj} - (\omega_1 - \omega_3)](\omega_{ij} - \omega_0)}. \quad (6)$$

This rearrangement is similar to, but not exactly the same as, that of Bloembergen *et al.*³

Figure 2 shows a single-sided diagram for the $\omega_1 + \omega_2 - \omega_3$ process. It is the only single-sided diagram for this process that has the same matrix elements as the terms in Eqs. (4)–(6). Figure 2 also shows the term corresponding to the single-sided diagram, which is identical to Eq. (4). That is, the term obtained from the single-sided diagram is identical to the principal term obtained after algebraic manipulation of the three double-sided diagrams. Indeed, Prior has verified for $\chi^{(3)}$ that the 24 principal terms generated by algebraically manipulating terms are precisely the terms obtained from the 24 single-sided diagrams.³⁷ This fact suggests rigorous general definitions of the words “principal term” and “correction term” in all orders. We therefore define principal terms to be those terms obtainable from single-sided diagrams (i.e., from perturbation theory in which damping is only included by allowing transition frequencies to become complex in the final result). All other terms required to yield the correct expression for the susceptibility will be called correction terms.

At this point, we introduce diagrams that give the correction terms in $\chi^{(2)}$ and $\chi^{(3)}$; they are described in detail in the Appendix. Two of these “trinomial-dephasing diagrams” are shown in Fig. 3 for the above $\chi^{(3)}$ process, and Fig. 4 shows diagrammatically the relationship between the double-sided, single-sided, and trinomial-dephasing diagrams for the three terms we have been considering for the $\omega_1 + \omega_2 - \omega_3$ process. In words, for $\chi^{(3)}$, a term from a single-sided diagram plus two terms from trinomial-dephasing diagrams sum to yield the three terms from the double-sided approach. Such a relation also holds for all other triplets of terms in $\chi^{(3)}$. The remaining 12 terms in the 48-term expression for $\chi^{(3)}$ can be rewritten using the remaining single-sided diagrams.

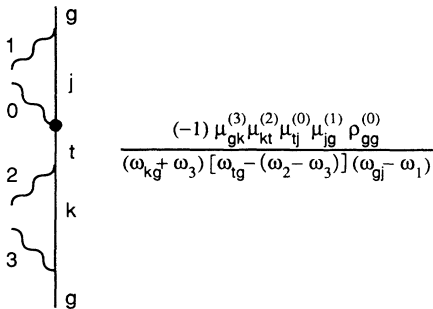


FIG. 2. A single-sided diagram for the $\chi^{(3)}$ process $\omega_0 = \omega_1 + \omega_2 - \omega_3$. A detailed description of the construction and interpretation of single-sided diagrams is given in Ref. 37.

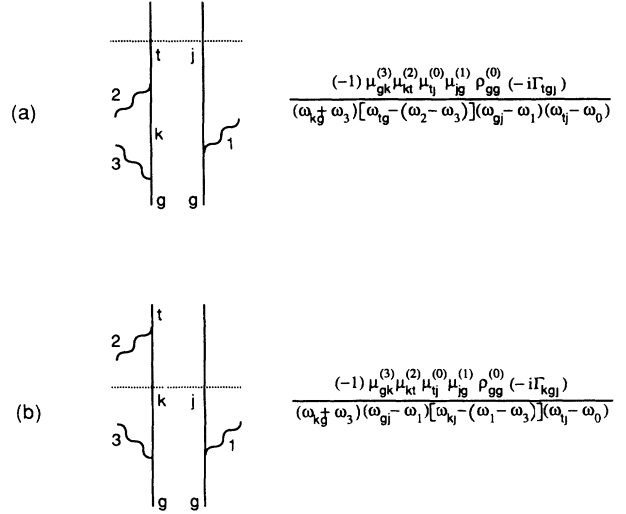


FIG. 3. (a) A trinomial-dephasing diagram and its corresponding term for the four-wave-mixing process $\omega_0 = \omega_1 + \omega_2 - \omega_3$. Observe that the term generated by this diagram is identical to the correction term given by Eq. (5). (b) The additional trinomial-dephasing diagram [obtained by sliding an interaction vertex from below to above the dashed horizontal line in (a)] and its corresponding term for the same four-wave-mixing process. Observe that the term generated by this diagram is identical to the other correction term given by Eq. (6). A detailed description of the construction and interpretation of trinomial-dephasing diagrams is given in the Appendix.

Thus, for the $\omega_1 + \omega_2 - \omega_3$ process, the sum of all of the terms obtained from double-sided diagrams equals the sum of all the terms obtained from single-sided diagrams plus all the terms obtained from trinomial-dephasing diagrams. Finally, since there is nothing unusual about the above third-order process, it is not difficult to see that the preceding statement is true for all third-order processes.

This algebraically rearranged set of terms is often preferable to the terms directly obtainable from the

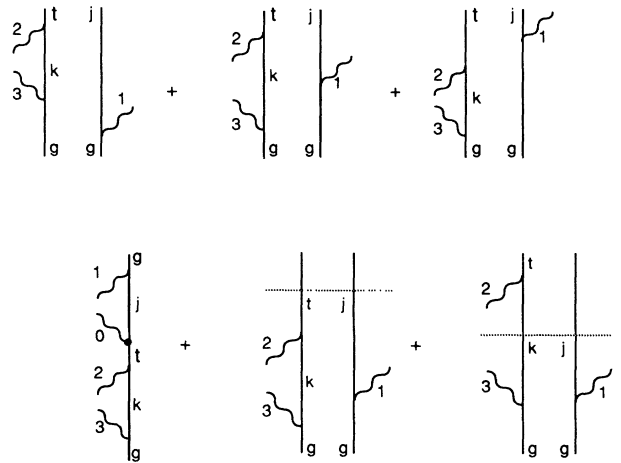


FIG. 4. Diagrammatic sum showing that three double-sided diagrams sum to yield one single-sided diagram and two trinomial-dephasing diagrams.

double-sided diagrams because it clearly separates trinomial-dephasing terms from principal terms. In addition to this conceptual advantage, there are other advantages as well to this arrangement. It should simplify some computations, which typically involve adding together many terms. Clearly much of the algebra required to describe trinomial-dephasing phenomena has already been done in deriving this arrangement. Also, for the case of very low pressure (i.e., weak dephasing) and long-lived populated states, correction terms do not contribute, which results in a reduction from $2^N N!$ to $(N+1)!$ terms for a given state ordering. Whether all state orderings are considered or not, the reduction is by a factor of $2^N(N+1)$ (see Table I), which is significant for $N \geq 3$. Neglect of all correction terms in this case should thus save considerable time and effort. In addition, as the pressure (dephasing) increases, correction terms can be included as a perturbation. Another advantage of this arrangement is that it better displays the relative strengths of correction terms themselves, since, within the set of correction terms, some are stronger than others. For example, dephasing between electronic levels is generally much stronger than within an electronic level (e.g., between Zeeman or hyperfine levels), so correction terms proportional to a trinomial-dephasing factor involving the former rates will generally be stronger than those involving the latter rates. (One should be careful, however, to consider resonant denominators, as well, in such determinations.)

It is, however, not obvious at this point whether single-sided diagrams plus trinomial-dephasing diagrams yield a result equivalent to that obtained with double-sided diagrams *in all orders*. Section IV is the proof that this is the case. For now, we precisely state the theorem that is the subject of this paper. In all orders, the nonlinear susceptibility in the standard approximations can be written as the sum of (1) all of the terms from single-sided diagrams, and (2) all of the trinomial-dephasing terms (all proportional to factors of the form, Γ_{ijk}), given by trinomial-dephasing diagrams. That is, in all orders, the set of all correction terms is equivalent to the set of all terms obtained from trinomial-dephasing diagrams.

This expansion is physically equivalent to the well-known expansion obtained using double-sided diagrams.

IV. PROOF

The proof is diagrammatic. That is, we will begin with the set of double-sided diagrams for an arbitrary order of the susceptibility, and, by manipulating them, we will show that the terms generated by them sum to the same value as do the terms generated by the single-sided diagrams plus the terms generated by the trinomial-dephasing diagrams. Since there is always a one-to-one correspondence between diagrams and mathematical terms, we use the words "term" and "diagram" interchangeably in this discussion.

We first point out that it is only possible to manipulate algebraically terms that all have the same matrix elements in their numerators; to do more would require special knowledge regarding the atomic system, which is only available in specific situations. We thus need to consider only the set of all N th-order double-sided diagrams that yield the same dipole-moment-matrix elements and density-matrix element. Henceforth, we refer to such a set of diagrams with the same dipole-matrix and density-matrix elements in the double-sided approach as a "class." Diagrams in the same class have the same states and photons on the bra (right) and the same states and photons on the ket (left). The relative heights of states and photons on the bra are the same for diagrams in the same class; the same can be said about the ket. Where diagrams within a class differ is in having different heights of interactions on *opposite* sides. For example, the diagrams in Fig. 1 form a class. In third order, there are 24 classes (for a given state ordering). Twelve contain three diagrams each, as that shown in Fig. 1, and the other 12 contain only a single diagram each. Diagrams in the latter set of classes are parametric;²² that is, they have all of their interactions on one side. In fifth order, where there are 3840 terms (for a given state ordering), there are 720 classes in all, with 240 containing ten diagrams, another 240 containing five, and another 240 containing one diagram each. As with $\chi^{(3)}$, diagrams in the last set

TABLE I. Number of diagrams (terms) for various orders before summing over state orderings or states. After the sum over state orderings is performed, the numbers of terms above must be multiplied by $(N+1)!$, yielding, for example, 1152 double-sided diagrams for $\chi^{(3)}$.

Order	Number of double-sided diagrams	Number of single-sided diagrams	Number of trinomial-dephasing diagrams	Fraction of terms due to trinomial-dephasing diagrams
$\chi^{(1)}$	2	2	0	0%
$\chi^{(2)}$	8	6	2	25%
$\chi^{(3)}$	48	24	24	50%
$\chi^{(5)}$	3840	720	3120	81%
$\chi^{(7)}$	645 120	40 320	604 800	94%
\vdots	\vdots	\vdots	\vdots	\vdots
$\chi^{(N)}$	$2^N N!$	$(N+1)!$	$(N+1)![2^N/(N+1)-1]$	$1 - [(N+1)/2^N]$ ($\rightarrow 1$ as $N \rightarrow \infty$)

of classes are parametric.

Since, it is only possible to manipulate algebraically diagrams within a class, we observe that it is sufficient to show that the single-sided-plus-trinomial-dephasing diagrammatic approach yields the same result as the double-sided approach *within each class of diagrams*. (It is also necessary to verify that the two approaches have a one-to-one correspondence of classes, but this is easily verified, recalling that the rules for the determination of matrix elements are identical for double-sided diagrams and trinomial-dephasing diagrams; see Table I.) This observation simplifies the calculations considerably.

We will need to separate all classes into two types. "Parametric" classes will be those containing only parametric diagrams. Such classes contain one diagram each. "Nonparametric" classes will be those containing only

nonparametric diagrams (with interactions on both sides). Nonparametric classes have more than one diagram each. Parametric and nonparametric classes comprise all classes and, hence, all diagrams, as well. This is because no class contains both parametric and nonparametric diagrams.

We begin by considering parametric classes. Figure 5 shows two generic diagrams representing two different parametric classes. Figure 5 also shows two single-sided diagrams. We immediately observe that the term generated by each double-sided diagram in Fig. 5 can be generated identically by a single-sided diagram. Thus each parametric double-sided diagram can be replaced by a single-sided diagram. This completes the part of the proof for parametric classes.

Now consider nonparametric classes. This case will require significantly more effort, occupying the remainder of this section, because all of the algebra occurs in these classes. Observe that, to generate an entire nonparametric class of diagrams from a given diagram, it is only necessary to move interactions up or down on each side, without changing the order of the interactions on a given side. Figure 6 shows a generic double-sided diagram for a class of diagrams corresponding to a $\chi^{(N)}$ process. We consider this diagram in detail during the remainder of this section. It has m interactions on the ket and m' interactions on the bra. In the figure, the order of interactions on a given side is determined, but no attempt has been made to distinguish relative heights between interactions on opposite sides because all possible orderings are intended to be represented by this diagram.

We now outline the remainder of the proof. We will derive the result that every nonparametric class of double-sided diagrams can be algebraically rewritten as an equal number of diagrams: *one* single-sided diagram

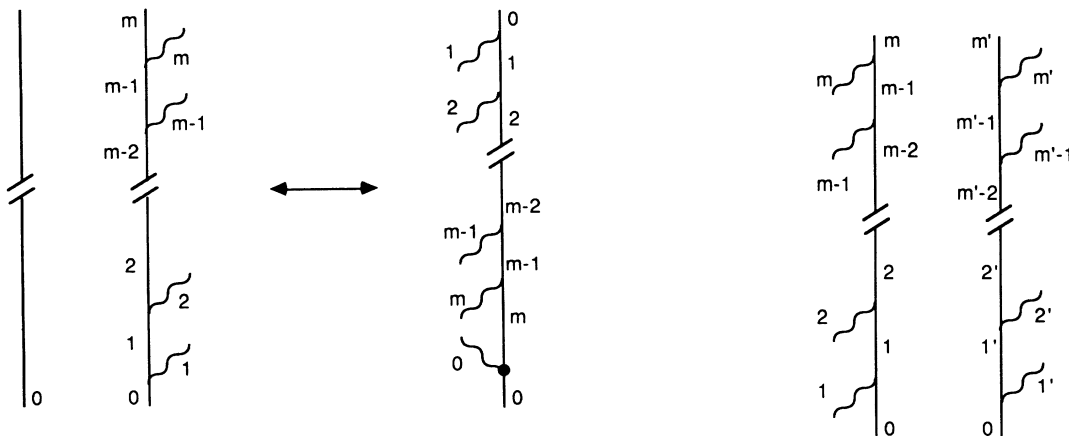
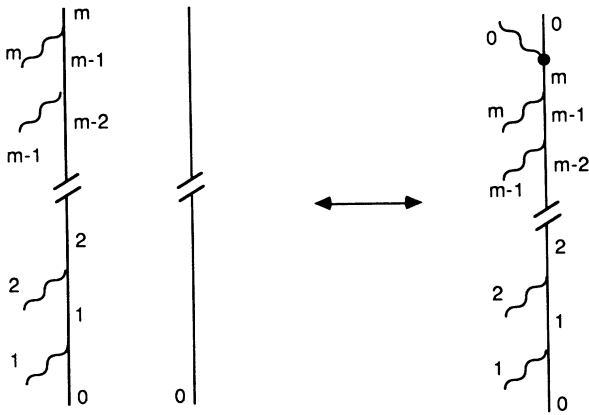


FIG. 5. Parametric double-sided diagrams and the corresponding single-sided diagrams that yield the same terms. In these diagrams, we have for simplicity drawn all input photons pointing upward to the right, i.e., as absorbed photons. It is clear, however, that the conclusions hold for emitted photons, also. (In Figs. 6–8 the same simplification is used.)

FIG. 6. Generic diagram for a class of double-sided diagrams for a $\chi^{(N)}$ process with m interactions on the ket and m' interactions on the bra ($N = m + m'$). While the order of the interactions on a given side is assumed to be the same for all diagrams in this nonparametric class, the relative order of interactions on opposite sides varies from diagram to diagram in the class.

plus its corresponding trinomial-dephasing diagrams. We will use the principle of mathematical induction. Our method will be to factor out a resonant-denominator factor involving the signal frequency from every term in a sum of terms generated from a nonparametric class of double-sided $\chi^{(N)}$ diagrams. This is equivalent to removing the uppermost interaction from each diagram. The remaining parts of all terms will then be written diagrammatically as those from two $\chi^{(N-1)}$ processes. Next, we will assume the theorem for all $\chi^{(N-1)}$ processes, as required by mathematical induction. This will allow us to replace expressions for each $\chi^{(N-1)}$ process with a single-sided $\chi^{(N-1)}$ diagram and its corresponding trinomial-dephasing $\chi^{(N-1)}$ diagrams. Performing a simple algebraic manipulation, we will find that the expression for the class of double-sided diagrams for the $\chi^{(N)}$ process can be written as one single-sided $\chi^{(N)}$ diagram plus a set of trinomial-dephasing $\chi^{(N)}$ diagrams. This will complete the inductive step, and examination of the lowest-order case establishes the initial step of the inductive process and completes the proof.

Before continuing, we define

$$\mathcal{D}^{(N)}(0; 1, 2, \dots, m; m', m' - 1, \dots, 1')$$

as the sum of terms over a class with the following state ordering: state 0 is the base state, states 1 through m are the states on the ket, reading upward, and states $1'$ through m' are the states on the bra, reading upward. The photon ordering is determined only on each side: as usual, within a class, the photon ordering on the bra is the same for all diagrams, as is the case for the ket; relative orderings of photons on opposite sides is where dia-

grams in this sum differ.

$$\mathcal{D}^{(N)}(0; 1, 2, \dots, m; m', m' - 1, \dots, 1')$$

is a function of the states, their ordering, and the light frequencies and polarizations. It is a sum over all possible relative heights of interactions on opposite sides of the diagrams. We suppress all arguments of $\mathcal{D}^{(N)}$ except for the states because, once the states are specified, the light frequencies and polarizations in our calculations will be clear from Fig. 6. It is also useful to define analogous sums over single-sided diagrams $\mathcal{S}^{(N)}$ and for trinomial-dephasing diagrams $\mathcal{T}^{(N)}$, where "classes" of these diagrams are defined analogously. The same conventions apply for the state arguments for $\mathcal{T}^{(N)}$, and for $\mathcal{S}^{(N)}$, the order of the state arguments is from bottom to top. [Of course, $\mathcal{S}^{(N)}(0; 1, 2, \dots, m; m', m' - 1, \dots, 1')$ consists of only a single diagram for all values of m and m' .] In this notation, then, the theorem can be stated:

$$\mathcal{D}^{(N)} = \mathcal{S}^{(N)} + \mathcal{T}^{(N)}, \quad (7)$$

where the state arguments of all three quantities in Eq. (7) are assumed to be the same:

$$(0; 1, 2, \dots, m; m', m' - 1, \dots, 1').$$

We now return to the class of diagrams containing the generic diagram shown in Fig. 6. We separate this class of diagrams into two subclasses, the first containing the diagrams having their uppermost interaction on the ket and the second containing all the diagrams having their uppermost interaction on the bra. We will break up the sum of all diagrams in the class into sums over these subclasses. $\mathcal{D}^{(N)}$ can then be written

$$\begin{aligned} \mathcal{D}^{(N)}(0; 1, 2, \dots, m; m', m' - 1, \dots, 1') = & \sum_{i=1}^{(N-1)!} \frac{(N-1)!}{(m-1)!m^i} (-1)^{m'} (\mu_{01}^{(1)} \cdots \mu_{m-1,m}^{(m)}) \mu_{mm'}^{(0)} (\mu_{m',m'-1}^{(m')} \cdots \mu_{1'0}^{(1')}) \rho_{00}^{(0)} \\ & (\omega_{mm'} - \omega_0) [\omega_{m-1,m'} - (\omega_0 - \omega_m)] \left[\prod_{j=1}^{N-2} d_{ij} \right] \\ & + \sum_{i=1}^{(N-1)!} \frac{(N-1)!}{m!(m'-1)!} (-1)^{m'} (\mu_{01}^{(1)} \cdots \mu_{m-1,m}^{(m)}) \mu_{mm'}^{(0)} (\mu_{m',m'-1}^{(m')} \cdots \mu_{1'0}^{(1')}) \rho_{00}^{(0)} \\ & (\omega_{mm'} - \omega_0) [\omega_{m,m'-1} - (\omega_0 - \omega_{m'})] \left[\prod_{j=1}^{N-2} d'_{ij} \right], \quad (8) \end{aligned}$$

where the first sum is over diagrams with the uppermost interaction on the ket and the second is over diagrams with the uppermost interaction on the bra. As required, each term contains the same matrix elements. In addition, each term in the first sum contains the two resonant denominators $(\omega_{mm'} - \omega_0)$ and $[\omega_{m-1,m'} - (\omega_0 - \omega_m)]$, which result from the two uppermost interactions. They have been explicitly written down; two similar factors have been written in the second term. The continued products represent different combinations of additional resonant denominators for each term. The only quantities varying from term to term in the sum are the additional resonant denominators d_{ij} and d'_{ij} , where d_{ij} (d'_{ij}) is the j th resonant denominator of the i th term of the first

(second) sum. No particular order of these resonant denominators or of the terms in the sum is specified, as none will be needed.

The critical step in this proof is the observation that, by factoring out the resonant denominator corresponding to the uppermost interaction from each term (i.e., by removing the uppermost interaction), we create two sums corresponding to two classes of diagrams for processes of order $N - 1$. (The matrix elements are slightly different, however. This is easily remedied by multiplying and dividing by the appropriate matrix elements.) Thus the sum of the $\chi^{(N)}$ diagrams in this class is equal to two sums of $\chi^{(N-1)}$ diagrams:

$$\begin{aligned} \mathcal{D}^{(N)}(0; 1, 2, \dots, m; m', m'-1, \dots, 1') &= \frac{\mu_{m-1, m}^{(m)} \mu_{m, m'}^{(0)}}{(\omega_{mm'} - \omega_0) \mu_{m-1, m}^{(0')}} \mathcal{D}^{(N-1)}(0; 1, 2, \dots, m-1; m', m'-1, \dots, 1') \\ &+ \frac{(-1) \mu_{m', m'-1}^{(m')} \mu_{m, m'}^{(0)}}{(\omega_{mm'} - \omega_0) \mu_{m, m'-1}^{(0')}} \mathcal{D}^{(N-1)}(0; 1, 2, \dots, m; m'-1, m'-2, \dots, 1'), \end{aligned} \quad (9)$$

where we have substituted $\mathcal{D}^{(N-1)}$'s for the appropriate sums. Observe that each $\mathcal{D}^{(N-1)}$ has different state arguments. In addition, we have temporarily defined polarizations ($0'$ and $0''$) and nonzero matrix elements ($\mu_{m-1, m}^{(0')}$ and $\mu_{m, m'-1}^{(0'')}$) for "signal" radiation of these lower-order processes. (These matrix elements have no physical significance and will cancel out later.) The factor of -1 in the second term comes about because there is one less interaction on the bra side of these lower-order diagrams than in the $\chi^{(N)}$ diagrams because the interaction factored out is on the bra.

We now use the principle of mathematical induction and assume the validity of the theorem for the value $N-1$, and proceed to demonstrate the validity of the theorem for the value N , using this assumption. Thus we can replace the sums of double-sided $\chi^{(N-1)}$ diagrams by the appropriate single-sided diagram and its corresponding trinomial-dephasing diagrams using $\mathcal{D}^{(N-1)} = \mathcal{S}^{(N-1)} + \mathcal{T}^{(N-1)}$. Having done this, we must next show that the above relation is also true for $\mathcal{D}^{(N)}$. The beauty of diagrammatic computations will be evident in the ease with which this is done.

To recreate diagrams for the $\chi^{(N)}$ process we multiply through by the matrix elements and resonant denominator that we removed earlier. This operation has the effect of adding back the interaction on the top of each trinomial-dephasing diagram that we removed earlier because, at the top, trinomial-dephasing diagrams are double sided and have an identical interpretation there as do double-sided diagrams. This operation creates all of the trinomial-dephasing diagrams for the $\chi^{(N)}$ process, except for the one with all interactions below the line. For the two single-sided diagrams, however, this operation does not yield the two $\chi^{(N)}$ single-sided diagrams, as required to prove the theorem, because single-sided-diagram interpretation is different from that of double-sided diagrams. Thus, we are left with two terms (the first two terms in Fig. 7), which must be shown to sum to the required single-sided $\chi^{(N)}$ diagram and the trinomial-dephasing diagram with all interactions below the line (the last two terms in Fig. 7). Doing some simple algebra, it is easy to verify that this is the case (see Fig. 7). As a result, we have shown, assuming that $\mathcal{D}^{(N-1)} = \mathcal{S}^{(N-1)} + \mathcal{T}^{(N-1)}$, it is also true that $\mathcal{D}^{(N)} = \mathcal{S}^{(N)} + \mathcal{T}^{(N)}$. This completes the inductive step.

For the final step, we must verify that the theorem is true for the lowest order. We may check the case $N=1$, where there are no trinomial-dephasing diagrams, and the susceptibility contains only single-sided diagrams. As a result, the theorem is trivially true for $N=1$. We must also verify the case $N=2$, however, because the inductive step of the proof is valid only for values of $N-1$ that have at least one trinomial-dephasing diagram; the

minimal case for which this is true, $N=2$, yields one trinomial-dephasing diagram in each nonparametric class. Checking this case is not difficult, and the theorem is proved.

V. COROLLARIES

(1) The most obvious and most important consequence of the new expansion is that dephasing-induced phenomena, and, specifically, trinomial-dephasing phenomena, exist in all orders of perturbation theory. In addition, interestingly, *all* of the correction terms, which give rise to these effects, are proportional to factors of the form Γ_{ijk} , and not a more complex expression. This result follows from rule (e) of the Appendix.

(2) A consequence of rules (c) and (e) that follows by inspection of the trinomial-dephasing diagrams is that any term proportional to Γ_{ijk} contains a resonance between the states i and k and is proportional to ρ_{jj} . Thus, while a trinomial-dephasing effect involves dephasing rates between all pairs of a set of three states, at least one of them

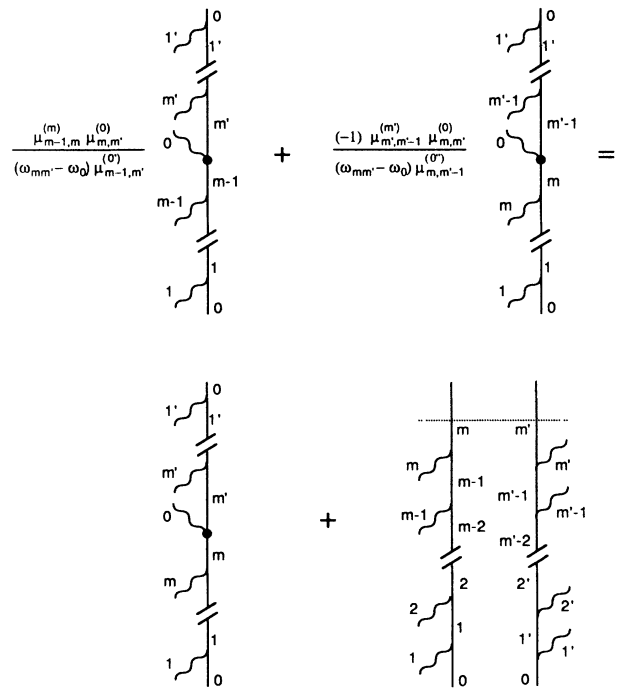


FIG. 7. Diagrammatic relation (required in the proof) showing that the two single-sided diagrams obtained from the $\chi^{(N-1)}$ processes in the mathematical induction process can be combined to yield the appropriate $\chi^{(N)}$ single-sided diagram and trinomial-dephasing diagram.

must be populated initially. Furthermore, the initially populated state is the state whose longitudinal relaxation may contribute to the strength of the effect. This is because of the γ_j term in $\Gamma_{ijk} = \gamma_j + (\Gamma_{ij}^{\text{pd}} + \Gamma_{jk}^{\text{pd}} - \Gamma_{ik}^{\text{pd}})$.

(3) Another result that follows easily is that, in all orders, resonances between initially unpopulated states are dephasing induced. To see this, observe that single-sided diagrams correspond only to terms with resonances involving the base state, which must be populated initially to contribute. Thus, resonances between initially unpopulated states can only originate from trinomial-dephasing diagrams, which carry the proportionality constant Γ_{ijk} . Of course, such resonances exist in all orders.

(4) Some results follow from the fact that trinomial-dephasing diagrams must have at least one interaction below the line on each side. Two-photon resonances between initially unpopulated states then must correspond to trinomial-dephasing diagrams with only one interaction on each side below the line, with the two initially unpopulated states of the resonance both occurring at the line. (The state at the base must be populated.) As a result, for two-photon resonances between initially unpopulated states, the states i and k in the factor Γ_{ijk} must represent the two initially unpopulated states. For three-photon resonances between initially unpopulated states, the third interaction may be above or below the line. Thus, for three-photon resonances between initially unpopulated states, only one of the states i or k must represent one of the initially unpopulated states of the resonance, although both may. And for four- or higher-photon resonances between initially unpopulated states, neither the state i nor the state k must necessarily be one of the relevant unpopulated states, although one or both may.

(5) Finally, as the order increases, the fraction of the terms that are trinomial-dephasing terms approaches 100%. Table I enumerates the terms and diagrams for various orders, neglecting different state orderings. Note that the total number of diagrams for a given order increases as $2^N N!$, while the number of single-sided diagrams increases only as $(N+1)!$. In fifth order, trinomial-dephasing terms comprise 81% of the terms; in seventh order, this fraction increases to 94%; in thirteenth order, it is 99.8%. The computational simplicity resulting when these terms can be neglected is evidently significant.

VI. DISCUSSION

In general, diagrammatic approaches to physical problems provide several benefits. They simplify algebra, give a clearer picture of the physics, and, in the cases of Feynman diagrams in quantum electrodynamics and other nonlinear-optical approaches, represent the quantum-mechanical time propagators in a relatively obvious way.³⁰ The approach described herein simplifies algebra and clarifies some physics, but trinomial-dephasing diagrams do not represent propagators in a simple manner. Instead, they represent partial sums of propagators, rather than individual propagators as in the usual approach. This is, of course, a necessary result of the need to describe trinomial-dephasing effects. The propagators

summed in a given trinomial-dephasing diagram are elements of the same nonparametric class that cancel identically (except for one principal term) in the limit of low pressure and infinite lifetime of the populated state(s). Thus trinomial-dephasing diagrams represent combinations of highly related propagators. For example, the top two double-sided diagrams of Fig. 1 contribute to the trinomial-dephasing diagram of Fig. 3(b), while all three double-sided diagrams of Fig. 1 contribute to the trinomial-dephasing diagram in Fig. 3(a). Thus trinomial-dephasing diagrams mix time orderings in a manner that is easily seen from their geometry.

It was hoped originally that this new approach would simplify the computation of expressions for dephasing-induced ground-state resonances. This is not the case. The reason for this failure is quite interesting, however. Trinomial-dephasing diagrams represent effects that result from the addition of potentially many double-sided diagrams having the same photons on the bra and the same photons on the ket. It is the time orderings of the photons that differ (see Fig. 1). Ground-state resonances, on the other hand, represent the antithetical situation. Here, pairs of diagrams add together, one of which has its lowest (earliest) two photons on the bra, while the other has them on the ket. In addition, these two diagrams maintain the *same* photon time orderings (see Fig. 8). Another difference between these two types of effects is that the former involves terms from a single state ordering; the latter involves two terms from different state orderings. Consequently, the algebra used to generate trinomial-dephasing terms is not useful for generating expressions for ground-state resonances in any order. Indeed, it is not difficult to check that double-sided diagrams are better than trinomial-dephasing diagrams for calculating expressions for ground-state resonances. These observations reflect the physics that distinguishes ground-state resonances from initially unpopulated-state

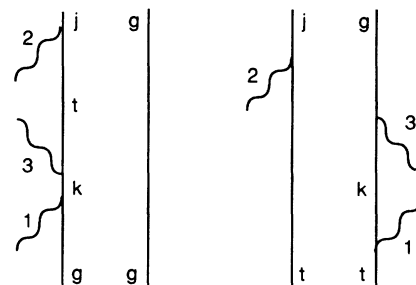


FIG. 8. Two double-sided diagrams that combine to yield ground-state resonances between states g and t . Note that these diagrams differ mainly in that the lowermost two interactions appear on the bra on one and on the ket on the other. Note that the time ordering of the photons is the same on each diagram. This is the antithesis of the situation that occurs in the generation of the terms that yield initially unpopulated-state resonances, in which all diagrams have the same interactions on their bras and kets but different time orderings of the interactions appearing on opposite sides (see Fig. 1).

resonances, which, in contrast, are more naturally described by trinomial-dephasing diagrams.

A natural question that arises is whether the expansion derived in this work can be generalized. Double-sided diagrams are useful in two regimes: (1) in the standard approximations and (2) in the more general integral regime, wherein these approximations are not made, and different rules are used for interpretation (see Sec. II). While the rearrangement of the double-sided diagrams is algebraically straightforward in the standard approximations, generalization of this approach to the more general integral regime does not appear to be so straightforward. The algebraic operation³⁹ that makes this rearrangement simple (see Ref. 4) depends on the precise mathematical form of the resonant denominators, which results from the standard approximations. If it is possible to rearrange the terms of the more general multiple integrals over propagators and perturbation Hamiltonians in the spirit of approach of this work, then the relaxation-induced component of the physics will be isolated from the non-relaxation-induced component in a general result. We are at present considering the possibility of this generalization.

The assumptions made in this work require that relaxation involving off-diagonal density-matrix elements be limited to a simple decay of coherence. More general relaxation processes have, however, been considered and observed. Coherence cross-relaxation effects, in which coherence between levels i and j decays to coherence between levels k and l or to another state m , can be considered.^{40–43} Extension of this approach to these more general regimes may be possible. Most likely, dephasing-induced phenomena will not be represented by such simple expressions in this more general regime.

VII. CONCLUSIONS

In conclusion, we have developed a new perturbative expansion for nonlinear optics and, with it, we have shown that dephasing-induced phenomena exist in all orders of the nonlinear-optical susceptibility. In this expansion, the N th-order nonlinear-optical susceptibility is written as the sum of two types of terms: (1) principal terms, obtained from single-sided diagrams, and (2) correction terms, obtained from a new type of diagram that we call a trinomial-dephasing diagram. In all orders, the correction terms are proportional to trinomials of dephasing rates, $\Gamma_{ijk} \equiv \Gamma_{ij} + \Gamma_{jk} - \Gamma_{ik}$. This approach reveals some general properties of dephasing-induced phenomena in all orders, and it appears useful for calculations of dephasing-induced phenomena, especially in higher order, where the number of terms is large.

ACKNOWLEDGMENTS

I would like to thank Larry Rahn for his insight and many suggestions. In addition, I am grateful for helpful comments from Professor Gilbert Grynberg, and Professor Girish Agarwal, who also kindly provided advance copies of his publications. This work was supported by the U.S. Department of Energy, Office of Basic Energy Sciences, Chemical Sciences Division.

APPENDIX: TRINOMIAL-DEPHASING DIAGRAMS

Trinomial-dephasing diagrams look much like double-sided diagrams and are constructed like double-sided diagrams, except for a (dashed) horizontal line, which separates trinomial-dephasing diagrams into two regions. At and above the line, the rules for interpreting double-sided diagrams are used. Below the line, however, rules for interpreting single-sided diagrams are used. Thus relative heights of interactions on opposite sides below the line are not important. Another distinguishing feature of the interpretation of trinomial-dephasing diagrams is that a factor of $-i\Gamma_{ijk}$, where j is the state at the base of the diagram and i and k are the states at the line, multiplies each term corresponding to a trinomial-dephasing diagram.

To construct a trinomial-dephasing diagram is quite simple: draw a double-sided diagram, and draw a horizontal line across it, leaving below the line on each side as few as one interaction and as many as all of the interactions. Figure 3 shows two examples of trinomial-dephasing diagrams.

To write down a term in the N th-order susceptibility corresponding to a trinomial-dephasing diagram, we follow these rules.

(a) Ignoring the horizontal line, use the double-sided rules (see Prior³⁷) for determining the density-matrix element, the dipole-moment matrix elements, the constant, and the overall sign of the term. For the diagrams in Fig. 3, this rule yields the factor

$$(-1)[n/(2\hbar^{N-1})]\mu_{gk}^{(3)}\mu_{kl}^{(2)}\mu_{ij}^{(0)}\mu_{jg}^{(1)}\rho_{gg}^{(0)},$$

where n is the density, $\mu_{\alpha\beta}^{(\gamma)}$ is the dipole-matrix element between states α and β for the polarization of the beam at ω_γ , and $\rho_{gg}^{(0)}$ is the ground-state population density.

(b) For interactions below the horizontal line, write down one resonant denominator for each state using the single-sided-diagram rules (see Prior³⁷). A slight variation must be remembered, however. For states on the bra (right) side, we now define the transition frequency of the resonant denominator by taking the frequency difference between the base state and the state above the interaction on the bra, rather than vice versa, as in the usual single-sided diagrams. Thus, on the bra, the order of the subscripts on the transition frequency is the reverse of that used for states on the ket. For the diagram in Fig. 3(b), this rule generates the factor $(\omega_{kg} + \omega_3)$ for the interaction on the ket and $(\omega_{gj} - \omega_1)$ for the interaction on the bra. For the diagram in Fig. 3(b), this rule yields the resonant denominators $(\omega_{kg} + \omega_3)$ and $(\omega_{gj} - \omega_1)$.

(c) Use the rules for double-sided diagrams to write down a resonant denominator for the interaction formed by the two states active at the dashed line. In Fig. 3(b) this rule yields the resonant denominator $[\omega_{kj} - (\omega_1 - \omega_3)]$.

(d) In addition, use the usual double-sided-diagram rules (ignoring the dashed line) to write down the resonant denominators for interactions above the dashed line. For the diagram in Fig. 3(b), the resonant denominator for the interaction above the dashed line is $(\omega_{ij} - \omega_0)$.

(e) Now multiply this result by the correction factor

$-i\Gamma_{ijk}$, in which i is the active state at the dashed line on the ket, j is the base state, and k is the active state at the dashed line on the bra. This rule gives the factor ($-i\Gamma_{kgj}$) for the diagram in Fig. 3(b).

As with other diagrammatic approaches,^{29,30,37} all transition frequencies $\omega_{\alpha\beta}$ are understood to be complex, that is, to include the dephasing rate between α and β : $\omega_{\alpha\beta} \rightarrow \omega_{\alpha\beta} - i\Gamma_{\alpha\beta}$.

To calculate the N th-order susceptibility in this ap-

proach, the terms obtained from trinomial-dephasing diagrams should be added to those obtained from the single-sided diagrams for the given process. As with the other approaches, it is also necessary to sum over all photon orderings and state orderings. An additional summation occurs if other states can contribute; if so, we must sum over all possible sets of $N + 1$ states.

For simplicity, we have omitted the constant factor $[n/(2\hbar^{N-1})]$ from expressions in the text.

- ¹N. Bloembergen, *Nonlinear Optics* (Benjamin, New York, 1965).
- ²C. Flytzanis, in *Quantum Electronics*, edited by H. Rabin and C. L. Tang (Academic, New York, 1975), Vol. 1, Pt. A.
- ³N. Bloembergen, H. Lotem, and R. T. Lynch, *Indian J. Pure Appl. Phys.* **16**, 151 (1978).
- ⁴R. T. Lynch, Jr., Ph.D. dissertation, Harvard University, Cambridge, MA, 1977.
- ⁵G. Grynberg, *J. Phys. B* **14**, 2089 (1981).
- ⁶Y. Prior, A. R. Bogdan, M. Dagenais, and N. Bloembergen, *Phys. Rev. Lett.* **46**, 111 (1981).
- ⁷A. R. Bogdan, Y. Prior, and N. Bloembergen, *Opt. Lett.* **6**, 82 (1981).
- ⁸L. J. Rothberg and N. Bloembergen, *Phys. Rev. A* **30**, 2327 (1984).
- ⁹A. R. Bogdan, M. W. Downer, and N. Bloembergen, *Opt. Lett.* **6**, 348 (1981).
- ¹⁰L. J. Rothberg and N. Bloembergen, *Phys. Rev. A* **30**, 820 (1984).
- ¹¹D. Grandclément, G. Grynberg, and M. Pinard, *Phys. Rev. Lett.* **59**, 40 (1987).
- ¹²G. Grynberg, E. Le Bihan, and M. Pinard, *J. Phys. (Paris)* **47**, 1321 (1986).
- ¹³G. Grynberg and P. Verkerk, *Opt. Commun.* **61**, 296 (1987).
- ¹⁴E. Giacobino and P. R. Berman, *Phys. Rev. Lett.* **58**, 21 (1987).
- ¹⁵G. S. Agarwal, *Opt. Commun.* **57**, 129 (1986).
- ¹⁶J. L. Carlsten, A. Szöke, and M. G. Raymer, *Phys. Rev. A* **15**, 1029 (1977).
- ¹⁷S. Reynaud and C. Cohen-Tannoudji, in *Laser Spectroscopy V*, edited by A. R. W. McKellar, T. Oka, and B. P. Stoicheff (Springer-Verlag, Berlin, 1981), and references therein.
- ¹⁸S. Le Boiteux, D. Bloch, and M. Ducloy, *J. Phys. (Paris)* **47**, 31 (1986).
- ¹⁹W. Lange, R. Scholz, and A. Gierulski, and J. Mlynek, in *Laser Spectroscopy VI*, edited by H. P. Weber and W. Luthy (Springer-Verlag, Berlin, 1983).
- ²⁰W. Lange, *Opt. Commun.* **59**, 243 (1986).
- ²¹Y. H. Zhou and N. Bloembergen, *Phys. Rev. A* **33**, 1730 (1986).
- ²²M. S. Kumar and G. S. Agarwal, *Phys. Rev. A* **33**, 1817 (1986).
- ²³G. S. Agarwal and N. Nayak, *Phys. Rev. A* **33**, 391 (1986).
- ²⁴G. S. Agarwal, *Opt. Lett.* **13**, 482 (1988).
- ²⁵M. Dagenais, *Phys. Rev. A* **24**, 1404 (1981).
- ²⁶M. Dagenais, *Phys. Rev. A* **26**, 869 (1982).
- ²⁷R. Trebino and L. A. Rahn, *Opt. Lett.* **12**, 912 (1987); R. Trebino and L. A. Rahn, in *Laser Spectroscopy VIII*, edited by S. Swanberg and W. Persson (Springer-Verlag, Berlin, 1987).
- ²⁸L. A. Rahn and R. Trebino (unpublished).
- ²⁹S. Y. Yee, T. K. Gustafson, S. A. J. Druet, and J. -P. E. Taran,

Opt. Commun. **23**, 1 (1977).

³⁰T. K. Yee and T. K. Gustafson, *Phys. Rev. A* **18**, 1597 (1978).

³¹J. F. Ward, *Rev. Mod. Phys.* **37**, 1 (1965).

³²G. L. Eesley, *J. Quant. Spectrosc. Radiat. Transfer* **22**, 507 (1979).

³³Ch. Bordé, in *Advances in Laser Spectroscopy*, edited by F. T. Arecchi, F. Strumia, and H. Walther (Plenum, New York, 1983).

³⁴J. Bordé and Ch. J. Bordé, *J. Mol. Spectrosc.* **78**, 353 (1979).

³⁵A. Omont, E. W. Smith, and J. Cooper, *Astrophys. J.* **175**, 185 (1972).

³⁶S. A. J. Druet and J. -P. E. Taran, *Prog. Quantum Electron.* **7**, 1 (1981).

³⁷Y. Prior, *IEEE J. Quant. Electron.* **QE-20**, 37 (1984).

³⁸J. Liu, J. T. Remillard, and D. G. Steel, *Phys. Rev. Lett.* **59**, 779 (1987).

³⁹There is a decision procedure that yields the rearrangement. It is as follows: Always combine pairs of terms. Begin by finding a pair of terms that have all but one resonant denominator in common. It is also necessary that the two noncommon resonant denominators contain transition frequencies of the form ω_{ij} in one and ω_{jk} in the other, where the common state j is the state at the base of the diagrams. As a result, the sum of these two terms will be proportional to the sum of the two noncommon denominators:

$$\begin{aligned} & \left[\omega_{ij} - \sum_i \omega_i \right] + \left[\omega_{jk} - \sum_j \omega_j \right] \\ & = \omega_{ik} - \sum_i \omega_i - \sum_j \omega_j - (i\Gamma_{ij} + i\Gamma_{jk} - i\Gamma_{ik}) \\ & = \left[\omega_{ik} - \left[\sum_i \omega_i + \sum_j \omega_j \right] \right] - i\Gamma_{ijk}, \end{aligned}$$

where $\sum_i \omega_i$ and $\sum_j \omega_j$ are the sums of input light frequencies in the two noncommon denominators. Also, as usual, we interpret all of the transition frequencies to be complex, containing implicit terms equal to $-i\Gamma_{\alpha\beta}$. From this simple manipulation, it is easy to see that trinomial-dephasing terms result. It is also possible to find the decision procedure for which pairs of terms to combine, and in what order, for any given wave-mixing process.

⁴⁰M. S. Kumar and G. S. Agarwal, *Phys. Rev. A* **35**, 4200 (1987).

⁴¹W. Gawlik, *J. Phys. B* **10**, 2561 (1977).

⁴²M. I. Dyakonov and V. I. Perel, *Opt. Spektrosk.* **20**, 472 (1966) [*Opt. Spectrosc. (USSR)* **20**, 257 (1966)].

⁴³C. Cohen-Tannoudji, *Applications of Lasers in Atomic and Molecular Physics*, Proceedings of Les Houches Summer School of Theoretical Physics, 1975, edited by R. Balian, S. Haroche, and S. Liberman (North-Holland, Amsterdam, 1976).